Arabian Journal of Geosciences (2022) 15:1593
https://doi.org/10.1007/s12517-022-10867-z

ORIGINAL PAPER

Mangrove forests mapping using Sentinel-1 and Sentinel-2 satellite images

Alireza Sharifi[1] · **Shilan Felegari**[2] · **Aqil Tariq**[3,4]

Received: 16 March 2022 / Accepted: 17 September 2022 / Published online: 6 October 2022

Abstract

Mangrove forests in West Asia are pure and sparse to dense communities in contact with high salinity. However, they have been rapidly declining during the previous two decades. What is critical to understanding the growth of mangrove species and better assessing the value of their ecological services is the knowledge gained about mangrove mapping. Since mangrove forests grow primarily in tropical and subtropical regions, and in these areas, the sky is usually cloudy, we used a combination of Sentinel-1 and Sentinel-2. A random forest algorithm is used to investigate the potential of Sentinel images for the extraction of mangrove forests in southern Iran, and seven spectral indices were used for better monitoring of mangrove forests. Our research was focused on three questions: (1) For mangrove forests mapping, whether Sentinel imagery, Sentinel-1 SAR data, or Sentinel-2 multispectral data, is more accurate; (2) which Sentinel imaging feature combination produces the best appropriate mangrove forests map; (3) how does a 10-m resolution map increase our understanding of the distribution of mangrove forests when compared to 30-m resolution mangrove products obtained from Landsat imagery? This study showed that the Sentinel-2 time-series images with an F1-score (0.89) are more effective in extracting the mangrove map than the Sentinel-1 time-series images with an F1-score (0.83). According to this study, it can be stated that the combination of multispectral and SAR images had an acceptable performance in separating areas with an area of less than 1 hectare of mangrove forests.

Keywords Mangrove forests · Sentinel-1 · Sentinel-2 · Google earth engine · Random forest

Introduction

Mangroves are trees or bushes that grow on low-sloping, fine-grained tropical tides and estuaries and have adapted to life in saline water and flooding. Mangrove forests are distributed in the tropics and subtropics, between 30° North and 20° South (Jia et al. 2019). The extent global of mangroves is estimated at 16 to 18 million hectares, found in various parts of West, South, and East Asia; Australia; the USA, West Africa; and the Middle East, and in most habitats are distributed as pure mangrove communities in the form of separate and integrated thin to dense stands with a short to medium height (Robertson et al. 1991). The development of surface roads, oil pollution caused by tanker traffic or maritime accidents, the discharge of oil effluents, unbalanced tourism activities, and the development of aquaculture in their vicinity threaten these areas (Jia et al. 2020). The extent of mangrove forests is endangered and is declining significantly, so the complete extinction of these areas in the next 100 years is not out of the question. For effective resource management today, it is essential to know the extent and position of resources and how they have changed over time (Twilley et al. 2018). Ecological studies now require biophysical and habitat data over time for specific areas, and remote sensing will make these studies easier (Felegari et al. 2021; Ghaderizadeh et al. 2021).

Responsible Editor: Biswajeet Pradhan

✉ Alireza Sharifi
a_sharifi@sru.ac.ir

[1] Faculty of Civil Engineering, Department of Surveying Engineering, Shahid Rajaee Teacher Training University, Tehran, Iran

[2] Faculty of Agriculture, Department of Soil Science, Zanjan University, Zanjan, Iran

[3] State Key Laboratory of Information Engineering in Surveying Mapping and Remote Sensing, Wuhan University, 430079 Wuhan, China

[4] Department of Wildlife, Fisheries and Aquaculture, Mississippi State University, 775 Stone Boulevard, Mississippi State, MS, USA

Remote-sensing detection can provide a good tool for monitoring extensive mangrove forests, often difficult to access (Tan et al. 2010). Remote-sensing techniques quickly show reductive and destructive changes, so it is possible to identify the threat factor and the driving force of destruction and risk management in the mangrove ecosystems (Azmat et al. 2020; Tariq et al. 2022). This identification is more efficient in a more detailed examination because instead of examining the entire study area, some of the degraded areas can be discussed. Images used to detect changes in mangrove forests are divided into two groups: single-date and multi-date (Sidik et al. 2018). Because all images from the mangrove region must be obtained at tide time from the region, which is difficult to provide, large-scale single-date approaches are difficult to employ (Mursyid et al. 2021). It has also made it difficult to use this technique in single-date images due to the spectral similarity of vegetation with mangroves (Camisón and Villar-López 2014). The images used in the single-date method are mostly optical images or SAR images, or a combination of both. The problems mentioned in the single-date method are solved to an acceptable extent with using the multi-date method (Hu et al. 2021).

Since the Sentinel-1 and Sentinel-2 images became available with the launch of the two satellites in 2014, changes in the mangrove forests have been noticeable because the Sentinel-1 signal can penetrate through clouds and obtain useful data (De Alban et al. 2020). Also, 4 of the 13 bands of Sentinel-2, which are highly sensitive to plant biophysical properties such as water and chlorophyll content and have a resolution of 5 days, are suitable for studying changes in mangrove forests (Hurskainen et al. 2019). Also, one of the advantages of using Sentinel images is the possibility of processing these images in the GEE (GEE) platform, because in this platform, the problems related to processing large volumes of data related to large-scale areas have been solved to an acceptable level (Zhang et al. 2019). Wessel et al. (2018) examined the capability of Sentinel-2 satellite imagery to distinguish coniferous, beech, and oak species in two forest areas in the German state of Bavaria. They showed images of different growing seasons during the year to increase the possibility of resolution of coniferous species of broadleaf were used, thus showing the high ability of Sentinel-2 images to classify tree species (Wessel et al. 2018). Akhrianti (2019), in the study of the spatial distribution of mangroves on Klapen Island using Sentinel-2 images, concluded that the analysis of Sentinel-2 images using GEE is very useful for analyzing the spatial distribution of mangroves and was able to distribute the mangrove space in Provide Valve Island in three classes (low, medium, and high) with an accuracy of approximately 86%.

Satellite image classification is the most common method of preparing cover or land use maps. In recent years, the application of new classification methods has been growing. In general, these methods can be divided into supervised and unsupervised categories based on the use or non-use of information such as ground data, aerial photographs, and satellite images by human agents. Supervised classification methods are divided into two groups: parametric and non-parametric. In parametric classification methods such as maximum probability and minimum distance to mean, statistical parameters such as mean and matrix and variance-covariance of educational data are used. The main problem with these methods is their dependence on the normal data distribution. For this reason, non-parametric methods such as random forest are used to classify satellite images. Random forest models are used as one of the modern models of machine learning in remote sensing (Thiagarajan et al. 2021). These methods have more robust results than many other classification methods on many platforms and databases. Random forest classification is also a training technique for decision trees using educational data. After creating the decision trees and executing the algorithm, the prediction result of each tree is determined separately. The classification output is the categories that have the most predictive results for trees. Random forest efficiency has been proven for extensive collections. Hence, it can be used to analyze satellite data (Badusha and Mohideen 2021). This method dramatically reduces the volume of data and has a high processing speed in classifying big data. The simple and understandable structure of the random forest algorithm makes it flexible and can be easily combined in other ways. It also has high speed and capability in areas that appear due to increasing educational samples of noisy data. Various studies have examined plant biomass prediction models using remote sensing data, such as Castillo et al. (2017), used Sentinel-2 multispectral images to develop biomass prediction models and machine algorithms to map mangrove forests biomass in the Philippines. Their findings revealed that red-edge bands (bands 4, 5, and 7) combined with altitude data were the best combination of variable sets for biomass prediction among the Sentinel-2 multispectral bands. They also claimed that Sentinel-1SAR and Sentinel-2 multispectral pictures might be useful for collecting and forecasting mangrove biomass maps.

Li et al. (2020) used Sentinel-2 multispectral data and high-resolution images from Google Earth as input data to map mangrove forests and classify these areas using vector algorithms off the coast of Shenzhen (Li et al. 2020). Their results showed that a combination of Sentinel-2 MSI and Google Earth images with an overall accuracy of 78.75% and a kappa coefficient of 0.74 has a high potential for mangrove map detection.

Mondal et al. (2021) attempted to monitor African mangrove forests using machine learning and satellite data. To do this research, they analyzed all Sentinel-1 and -2 data

on the GEE platform (Mondal et al. 2021). Their results showed that the combination of the machine learning group and Sentinel images was effective in mangrove monitoring, with high accuracy for all study areas in Africa (producer accuracy of 92% and 99%, user accuracy of 98% and 100%, and accuracy total 95% and 99%) were calculated.

Ghorbanian et al. (2021) used 81 data received from Sentinel-1 and 41 data received from Sentinel-2 to monitor the mangrove forests of Qeshm Island in southern Iran, and the data were analyzed by a random forest algorithm (Ghorbanian et al. 2021). The average overall accuracy and kappa coefficient of their output map was 92% and 0.93, respectively. Their research showed that the integration of multimedia remote sensing data and the use of seasonal features led to the production of a detailed map of mangrove forests. Toosi et al. (2022) used a random forest algorithm and remote sensing to classify the mangrove ecosystems on Qeshm Island in southern Iran. They concluded that based on the spectral and spatial characteristics of Sentinel-2, a mangrove forests classification map was presented. Using the design approach in their research resulted in an overall accuracy of 65.5% and a kappa coefficient of 0.63, creating the highest accuracy for classifying mangrove cover and deep water (Toosi et al. 2022).

Ronoud et al. (2021) tried to monitor mangrove forests on Qeshm Island in southern Iran using Sentinel-1 and -2 data. They used the *k*-nearest neighbor algorithm, which was highly accurate for such research. Using multiple linear regression (MLR) and *k*-NN algorithms, the best RMSE was 19% for S-1 and 17% for S-2. Vaiphasa et al. (2005) investigated the possibility of distinguishing between tropical mangrove species by using visible and near-infrared (NIR) channels of hyperspectral data (Vaiphasa et al. 2005). The reason for this is that electromagnetic radiation interacts with leaf constituents such as cellulose, lignin, water, protein, oil, and leaf structure.

In this study, we intend to use Sentinel-1/2 images to investigate and detect mangrove forests changes in the GEE platform. This study was conducted in the mangrove forests of the coastal areas of southern Iran. In summary, our objectives of this study are (i) investigating the changes of mangrove forests in 10 years on a suitable scale using the time-series images of Sentinel-1 and Sentinel-2 with a spatial resolution of 10 m and preparing a map of changes; (ii) study of mangrove forests changes using standard features of large-scale Sentinel-1 and -2 time-series data; (iii) comparing the quantitative and qualitative differences between the map prepared from the images of the time-series Sentinel-1 and Sentinel-2 with a spatial resolution of 10 m with other products in similar studies It can be said that almost all the studies related to the monitoring of mangrove forests in the GEE platform have been done to examine the extent of these forests. So far, the ability of this platform inaccurate mapping and detailed study of mangrove ecosystems has not been discussed. In addition, studies that have performed accurate mapping with this platform have practically used traditional approaches with several satellite observations. But in this study, we tried to provide high-quality and precise map by using open-access satellite images in GEE to maintain and manage this ecosystem and increase the level of digital automation in output production.

What will differentiate this research is the combination of Sentinel-1 and Sentinel-2 multi-source images for mangrove forests monitoring and ecosystem mapping on the GEE platform. Observing the time-series in this platform to reduce the tidal effect leads to the accurate mapping of this ecosystem without the need for tidal modification in the study area.

Materials and methods

Study area

Qeshm Island mangrove forests are located in the range of 26° 45′ to 27° north latitudes and 55° 20′ to 55° 51′ east longitude between Mehran and Gorzin river delta in the north of the Qeshm Island, and the closest point of the Qeshm Island is Left port to Khamir port. The Northwest of the mangrove reserve is about one kilometer and is located in the mangrove forests of the central Persian Gulf (Fig. 1). The average rainfall in this area is 114 mm, and the average annual temperature is 26.5°C.

The average annual maximum temperature and cold in this area are 30.1° and 22.3°C, respectively, with the maximum temperature recorded from May to July and the minimum temperature recorded from December to February (Mazraeh and Pazhouhanfar 2018). Table 1 shows the number of GPS points of the training samples of each class that were recorded in the study area. Also, the land use class of forest lands, non-forest swamps, tidal lands, and catchment lands were determined. Through the experts of the Mangrove Protection Organization, the area of each difference was determined in Table 2.

Satellite data

The integration of radar data with optical data can significantly improve image classification accuracy and differentiate the impermeability levels of land cover types. Sentinel-1 is a polar-orbiting satellite that performs radar imaging. The satellite implements microwave and C-wavelength ranges. The Sentinel-1 captures images from the earth in the C-radar band, capturing radar images with coverage of 400 km. Its polarity and

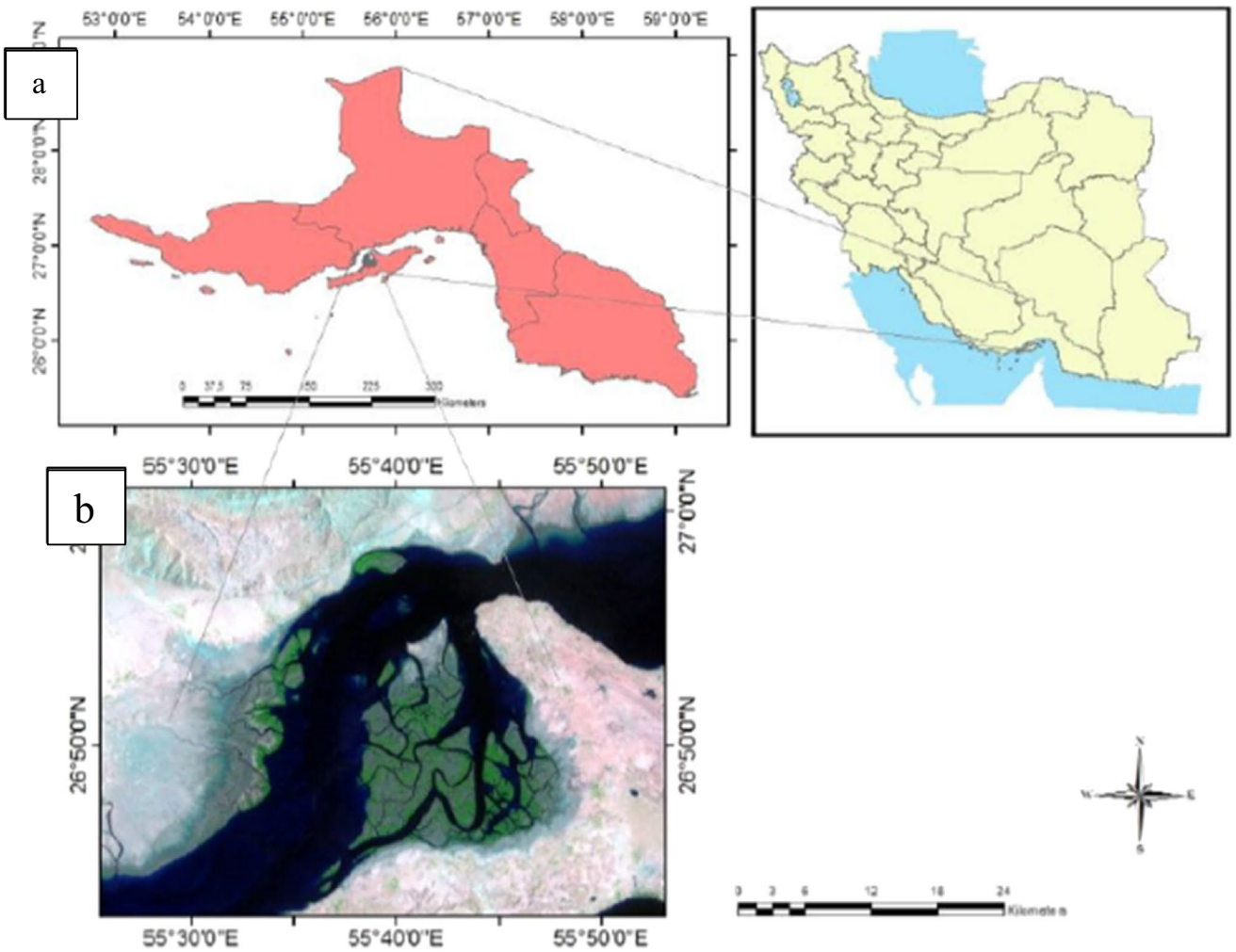

Fig. 1 **a** The study area, Hara Forest Protected Area, is located in the South of Iran, about 25 km northwest of Qeshm Island. **b** The Sentinel-2 image (true color composite) of the study area acquired on August 20, 2020

Table 1 GPS point of the five land cover classes

Land cover	Close canopy mangrove	Open canopy mangrove	Individual mangrove	Deep water	Mudflat
GPS point	44	38	23	41	63

Table 2 Area of land use classes in 2020 in the range of mangrove forests Island

Land use class	Forestlands	Non-forest swamps	Tidal lands	Catchment lands
Area (ha)	5512.69	7987.02	6326.50	5764.71

dual-polarization capability allow fast data delivery from the satellite to the ground station. In this study, Sentinel-1 data with two channels (VH and VV) were used. Sentinel-2 has a multispectral sensor called MSI and has a temporal resolution of 5 days at the equator and three days at mid-latitudes. The area covered by this satellite is from 84° north to 54° south. Sentinel-2 consists of 13 bands covering the range of visible, near-infrared, and short-wavelength infrared wavelengths (Karydas et al. 2020). The advantage of using Sentinel-1 and -2 data combinations is that mangrove forests grow primarily in tropical and subtropical regions, both of which are usually cloudy. Using data combination of these two sensors, we can have more precise images. It also increases the spectral properties of water and plants by calculating spectral indices. The seven spectral indices indicated in Table 3 was used in this study. The 10-m and 20-m bands are both available for the Sentinel-2, and changes must be made to the 20-m Sentinel-2 bands before generating spectral indices to access the 10-m split bands. The data used in this research were coded and analyzed on the GEE platform.

Table 3 Sentinel-2 (S-2) and Sentinel-1 (S-1) images yielded vegetation indices (VI)

Vegetation indices	Abbreviation	Equations	Source	Reference
Normalized difference vegetation index	NDVI	$\frac{\rho 842nm-\rho 665nm}{\rho 842nm+\rho 665nm}$	S-2	(Tucker 1979)
Normalized difference water index	NDWI	$\frac{\rho 842nm-\rho 1610nm}{\rho 842nm+\rho 1610nm}$	S-2	(Gao 1996)
Modified normalized difference water index	MNDWI	$\frac{\rho 560nm-\rho 1610nm}{\rho 560nm+\rho 1610nm}$	S-2	(Xu 2006)
Plant senescence reflectance index 1	PSRI1	$\frac{\rho 665nm-\rho 490nm}{\rho 705nm}$	S-2	(Hill 2013)
Plant senescence reflectance index 2	PSRI2	$\frac{\rho 665nm-\rho 490nm}{\rho 740nm}$	S-2	(Hill 2013)
Plant senescence reflectance index 3	PSRI3	$\frac{\rho 665nm-\rho 490nm}{\rho 783nm}$	S-2	(Hill 2013)
Plant senescence reflectance index 4	PSRI4	$\frac{\rho 665nm-\rho 490nm}{\rho 865nm}$	S-2	(Hill 2013)
Radar vegetation index	RVI	$\frac{\frac{VH}{VV}}{\frac{8*HV}{HH+VV+2\times HV}}$ $\frac{VH}{VV}$	S-1	(Hill 2013)

SAR data are beneficial for understanding the phenological characteristics of forests. Features such as moisture content, type of forest cover, and phenology can alter quantitative SAR values. RVI, which is a radar plant index, behaves similarly to optical spectral index. With the help of the RVI index, all the phenological features related to forest cover can be examined. Sentinel-1 data can be easily accessed on the Google Earth Engine platform.

One of the advantages of using this data in GEE is that there is no need to pre-process this data anymore, because GEE is a platform that can pre-process data before use and provide the required data to users (Chauhan et al. 2020). All preprocessors on this data include thermal noise removal, ground correction for each Sentinel-1 scene, border noise removal, file circuit correction, and radiometric calibration. We also use data from previous chapters (in the same period) and classify Sentinel-1 scenes.

To obtain the time-series data related to the studied scales, we use an average reducer. Using an intermediate reducer will reduce spot noise. We also used Sentinel-2 data, which is the same as high-atmosphere reflectance data, in this study, and all of the data can be used from the GEE platform. Pre-processing operations on Sentinel-2 images include cloud removal, and this cloud removal filter was performed on Sentinel-2 scenes with more than 5% cloud cover. An average reducer was also used for the Sentinel-2, the benefits of which include the removal of very bright spots, the removal of very dark spots, and the removal of clouds that provide access to clear Sentinel-2 scenes (Chauhan et al. 2020). Details about the number of Sentinel-1 and -2 images taken from the study area in different seasons are also presented in Table 4.

Methodology

The random forest (RF) algorithm is currently one of the best learning methods. This is a non-parametric machine learning algorithm based on a set of decision trees. Many decision trees grow in the classification of RF algorithms (Moradi and Sharifi 2022). Pixels or unclassified phenomena are included in a class according to their associated characteristics. The affiliation of the pixel to one of the classes (number of classes) among the decision trees is put to the vote, and each decision tree has its vote. The random forest method comprises a set of regression trees used to reconstruct training data. Usually, there are sets of samples that are randomly formed by replacing the original training data (Tucker 1979). Combining three parameters in a random forest method algorithm is essential: The first is how many trees should be made, the second is how many variables are involved in creating a node for each network, and the third parameter is the size of the node, which indicates the depth of the regression tree made. When a regression tree is made, a new instruction set is made by replacing the original instructional data set. The forest assigns the voted pixel to the class with the highest number of forest trees. Decision trees grow individually from the training sample set. With *N* substitution sampling, for training, about two-thirds of the original data set are used, and we represent the number of available samples with *n*. In this way, with alternative sampling, the remaining one-third of the

Table 4 Number of images used in each season of Sentinel-1 and -2 sensors

Season						
Data	Spring	Summer	Autumn	Winter	Total	Date
Sentinel-1	20	20	20	20	80	2020
Sentinel-2	11	11	12	7	41	2020

data will not be involved in tree training and will be set aside for internal validation of the algorithm. RF efficiency has been proven for extensive sets to be used for satellite data analysis (Sekulić et al. 2020). The samples were selected in two steps: (1) Sites with dimensions of 10 by 10 m were selected and tried to distribute adequately and evenly to the characteristics of the region, including other vegetation of the region, water, mangrove trees, agricultural lands, or imprevious surfaces; (2) areas that cover more than 30% of the mangrove area were called mangrove areas and areas with more than 70% non-mangrove cover including shrub areas, coastal areas, agricultural areas, water, and forest were called non-mangrove areas. To distinguish these areas from each other with the help of high-resolution images from Google Earth, mangrove and non-mangrove can be separated (Atwood et al. 2017).

To extract the mangrove, we used a combination of Sentinel time-series data. The Sentinel time-series data for this study are as follows: using Sentinel-1 data, using Sentinel-2 data, and a combination of Sentinel-1 and -2 data. As can be seen in Fig. 2, three scenarios were defined using Sentinel-1 SAR imagery (P1), Sentinel-2 imagery (P2), and a combination of Sentinel-1 and Sentinel-2 data (P3) to find out how sensitive the four red-edge bands of Sentinel-2 are to mangrove extraction. Using these two scenarios, we will determine the accuracy of the classification. In scenario P1, the extraction of mangrove forests is obtained by removing four red-edge bands. Still, in scenario P2, four red-edge bands are added, and the mangrove forests are extracted by these two scenarios.

Training and validation data

Spectral mixing is one of the most suitable methods for monitoring land cover in mangrove forests. This method is based on remote sensing, and can monitor the intertwined areas of mangrove forests well, because the spatial resolution of this method is very high. But with all the advantages of this method, it has significant disadvantages. This method requires pure pixels, because we need input data to be able to define pure pixels as input data, but pure pixels are complicated for real-world scenarios, which can be defined as input. To train and test machine learning classifications, reference sample data were prepared for both non-mangrove

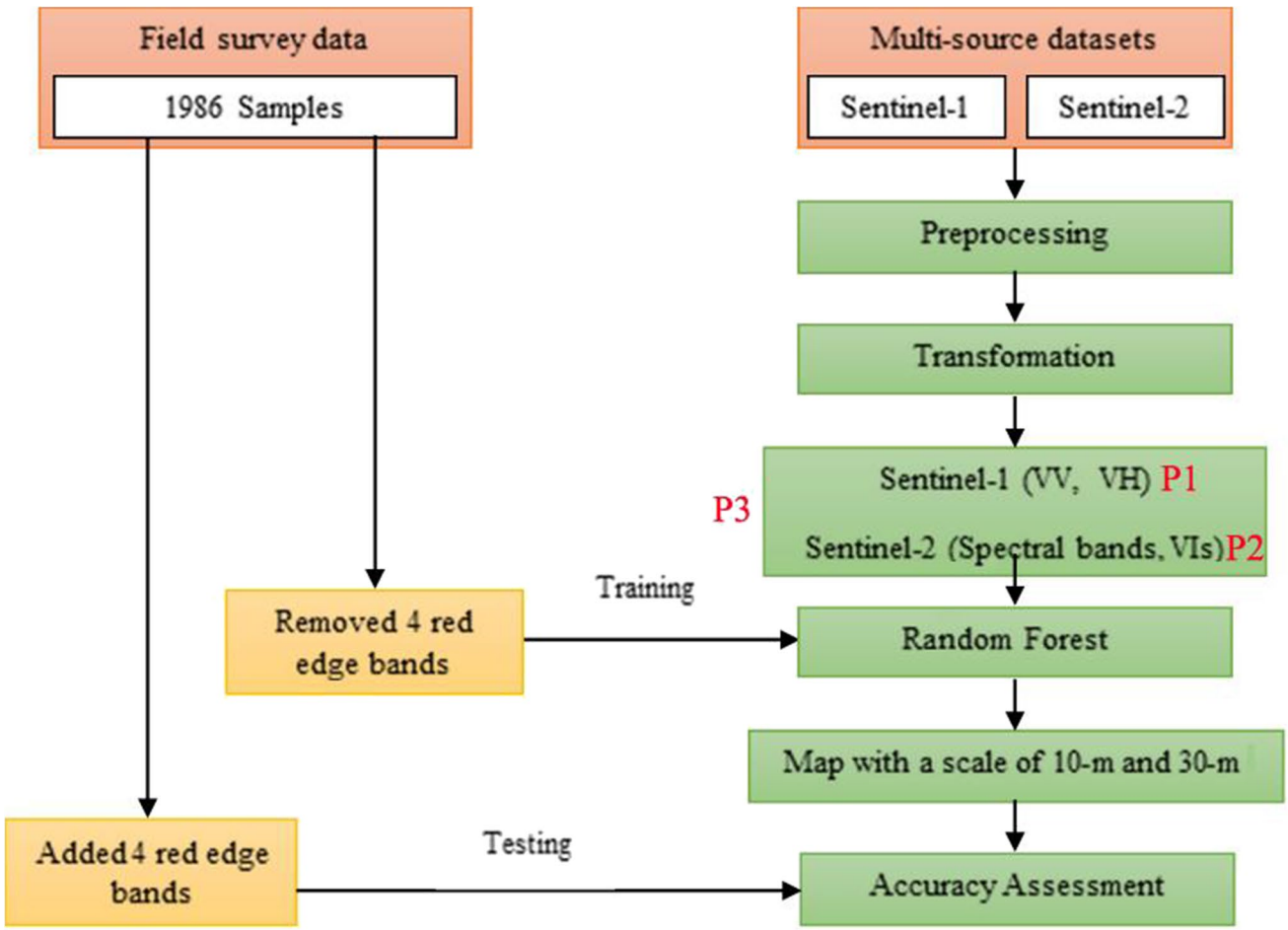

Fig. 2 Flowchart of the proposed method with three scenarios (P1, P2, and P3)

cover categories (including non-mangrove forests, water, bare land, settlements, crops, grasslands) and mangroves. (Sagawa et al. 2019).

Land use and land cover at the border of the image and geographical locations in coastal areas were evaluated, and a reference sampling site was considered for sample collection. Each mangrove sampling site will be detected when an area of 400 m^2 contains only mangrove trees (pure pixels). The same rule will apply to non-mangrove cover. In total, 4970 reference samples (2660 mangrove samples and 2310 non-mangrove samples) were used to map the mangrove forests only for machine learning model training, and 8204 reference samples (3970 mangrove samples and 4230 non-mangrove samples) were used only for evaluation. User accuracy in a classification map is defined when the pixel in question represents the class level, and the same pixel represents a particular class. A helpful indicator for assessing the level accuracy of the F1 rating class is the build accuracy, in which the probability of classifying a pixel as a specific class is examined. User's accuracy (U_A) and producer's accuracy (U_P) are two common indicators in assessing image classification accuracy (Wachid et al. 2017). By definition, the producer's accuracy is the probability of assigning a particular class to a pixel by a classification algorithm, provided that the actual class of that pixel is known to the manufacturer. This index is obtained by dividing the diameter element of each class in the error matrix by the sum of the column values of the same class. Also, the user's accuracy indicates the possibility of classifying a particular class according to the same class in the ground truth map, and in the error matrix for each class, which is obtained by dividing the diagonal element by the set of elements of the same class (Hu et al. 2018). The F1 unit is the average weight equalizer of the producer's accuracy is correct. These branches are calculated for class i as Eq. (1):

$$F1 = \frac{2 \times U_{Ai} \times P_{Ai}}{\left(U_{Ai} + P_{Ai}\right)} \quad (1)$$

The average accuracy of F1 is obtained from the arithmetic mean of F1 of the classes. The total accuracy is obtained from the sum of the elements of the original diameter of the error matrix divided by the total number of pixels.

Results

Map of mangrove forests on the Qeshm Island using images obtained from a combination of Sentinel-1 and Sentinel-2 data (P3), Sentinel-2 imagery (P2), and Sentinel-1 SAR imagery (P1), and it was prepared 1987 samples were used for validation, and F1 score, classification accuracy, user's accuracy, and producer's accuracy were calculated. In Table 2, the user and producer's accuracy were calculated from P1, P2, and P3 for the F1-score. The F1-score for P1, P2, and P3 was 0.87, 0.90, and 0.95, respectively. Producer's accuracy and user's accuracy were highest between P1, P2, and P3, indicating that using a combination of Sentinel-1 and -2 data reduces the error of increasing user's accuracy and increasing producer's accuracy in producing mangrove maps. In comparing the producer's accuracy between P1 and P2, this index was higher in P2 than in P1. According to this issue, it can be inferred that the map made from Sentinel-2 outputs provides a more accurate estimate than Sentinel-1 outputs from mangrove forests in the study area. Also, according to Table 5, the producer's accuracy of the P1 was less than that of the P2, which suggests that the Sentinel-2-derived map overestimated mangrove forests less than the Sentinel-1-derived map. Maps obtained from P1, P2, and P3 data were compared with Google Earth area images.

Figure 3 shows the performance of P1, P2, and P3 for mapping mangrove forests in the study area. Compared to the map prepared from P1 and P2, the map prepared from P2 had a higher estimate or area than the P1, which was consistent with the results of the accuracy assessment. In scenario P1, mangrove extraction was achieved by removing four red-edge bands, but in scenario P2 were added. The input features of P1 and P2 are (1) 15%, 20%, 40%, 55%, and 80% quantiles of NDWI, MNDWI, NDVI, longitude, latitude, aspect, slope, elevation, B2, B3, B4, B8, B11, B12, (2) 15%, 20%, 40%, 55%, and 80% quantiles of MNDWI, NDWI, NDVI, PSRI1, PSRI2, PSRI3, PSRI4; longitude, latitude, aspect, slope, elevation and B12, B11, B8A, B8, B7, B6, B5, B4, B3, B2. The distribution of mangrove forests in the Qeshm Island region was prepared using a 10-m map.

To prepare the distribution map, a combination of Sentinel-1 and Sentinel-2 dataset was used. According to the map, mangrove forests in 2010 were equal to 2400 ha. These forest areas are mainly spread on the edge of the island, located in the south of Iran (Fig. 4). The source of the 30-m mangrove maps is from Department of Environmental (Ghasemi et al. 2021). This map was obtained through the simultaneous use of Sentinel-1 and -2 data. After producing the classified map, a 30-m pixel size has been re-sampled; we examined the area of mangrove forests, which were less than

Table 5 The F1-score of each classification map derived from Sentinel-1 SAR imagery (P1), Sentinel-2 imagery (P2), and a combination of Sentinel-1and 2 data (P3) with related producer's and user's accuracies

Type	F1-score	Producer's accuracy	User's accuracy
P1	0.87	0.85	0.89
P2	0.90	0.91	0.90
P3	0.95	0.93	0.94

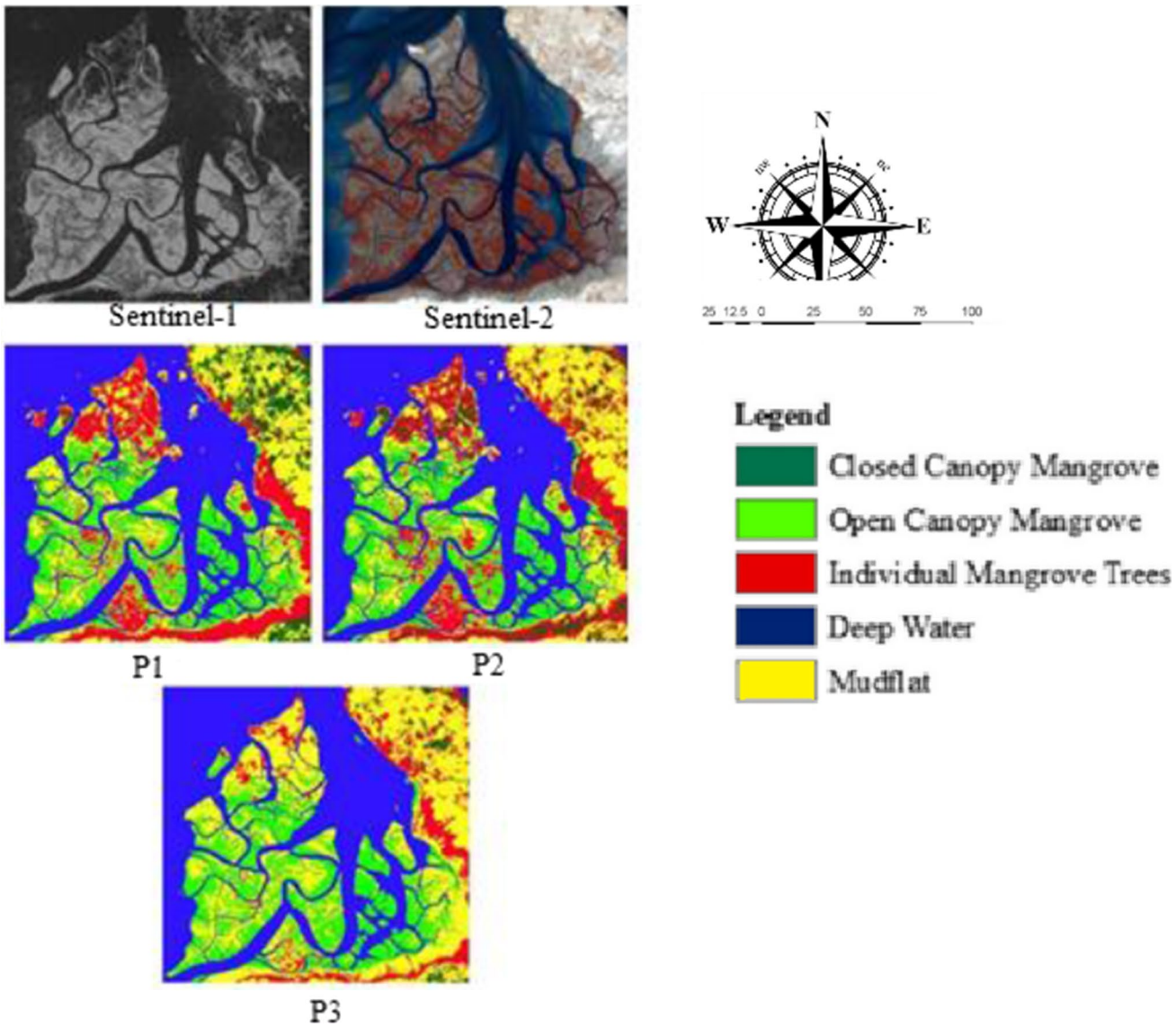

Fig. 3 Sentinel-1 (VH-polarized) and Sentinel-2 images (false-color composite: NIR-red-green) with related classification results derived from Sentinel-1 (P1), Sentinel-2 (P2), and a combination of Sentinel-1 and Sentinel-2 dataset (P3). The light green color represents the mangrove extraction results

1 ha in size and were scattered in heterogeneous and separate pieces, using Landsat images. The area of these separate areas was 300 ha, which accounted for 12.5% of the total area of mangrove forests in the study area, and 11,000 small pieces of mangrove forests were identified in the area.

The results showed that in the west of the region, there are a small number of small pieces of mangrove forest, which corresponded to the identification of mangrove pieces using a 10-m map, and these areas were identified accurately. A large number of mangrove forests in the west of the study area is probably due to human intervention in the ecosystem of this area, and activities such as land reclamation, aquaculture, and recreational and commercial boat traffic are among the causes of the fragmentation of mangrove forests in this region. We also compared the area of mangrove forests in the 0.1° networks with the 10-m and 30-m resolutions, respectively. This comparison showed that in the 10-m map, the area of mangrove forests was larger than the areas derived from the 30-m map.

Mangrove forests cover was high for both scenarios, which concluded the four red-edge bands in Sentinel-2 have a small share in the extraction of mangrove forests in the study area, but Scenario P2 has been more successful than scenario P1. Errors in the 10-m map of mangrove forests were revealed by examining the study area on Google Earth. One of the error maps is the 10-m map resulting from the simultaneous use of Sentinel-1 and -2 data. The main cause of these errors is the riverside and aquaculture ponds and

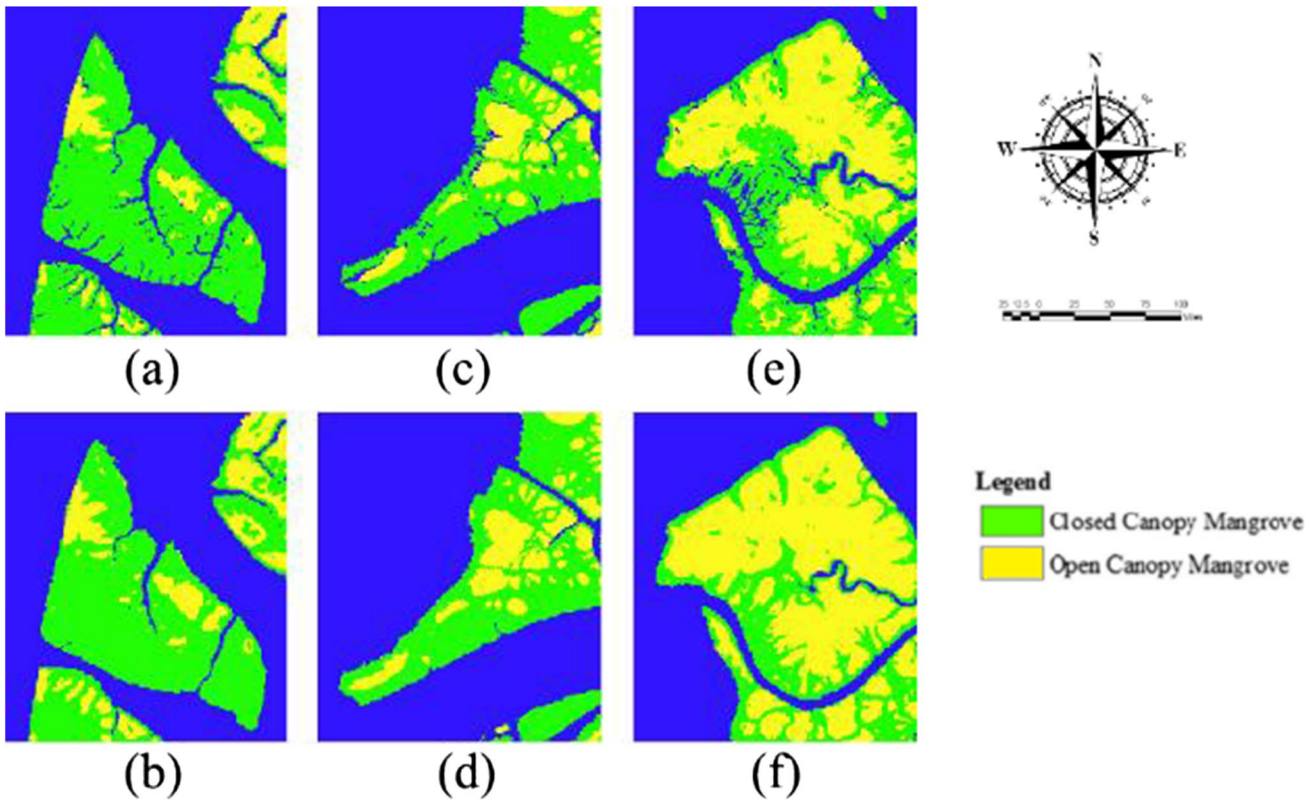

Fig. 4 Collation of 10-m and 30-m maps extracted from mangrove forests monitoring results

the evergreen plants of the region that cause errors in the classification pixels (Kumar and Mutanga 2018), because there is a spectral similarity between the mentioned items and their reflection in the classification results (Fig. 5).

According to Table 6, which shows the classification results, it can be stated that for the two scenarios, P1 and P2, the index reflects the accuracy of the class level, which is shown with the F1 score (the numerical value of F1 for P1 and P2 0.88 and 0.92, respectively).

This study shows that no distinction exists between mangrove and water cover and evergreens, the overlap between the intensity of two spectral bands (such as SWIR-1 in Fig. 6a, b), and the amplitude of two channels (VV and VH in Fig. 6c, d). and. Therefore, it can be said that there is no difference between the river bank and evergreen plants with mangrove cover, and even this error in Landsat images is irreparable in both 10-m and 30-m maps (Friess et al. 2019), and we should seek to identify factors to enable the resolution of such errors in future research. A locally scale (10 m) map of mangrove forests provided by Sentinel images provides more accurate information than a 30-m map, especially of individual mangrove forests plots.

In previous studies, a mangrove forests map was prepared with Landsat images at a 30-m scale. Due to the lack of details, we could not have a more accurate performance of this particular ecosystem (Osland et al. 2016; Van der Stocken et al. 2019), and we could not speak with confidence in estimating the carbon reserves of these areas.

Discussion

One of the most up-to-date research topics is research on areas where the spectral information of phenomena is similar to each other, and the purpose of such study is to improve and enhance satellite image classification methods. Also, to improve land cover maps in the forestry sector, the focus is on research that combines satellite data with different spatial resolutions. Mangrove trees cover a large area of the Earth's surface and develop aerial roots for better physiological function. Because they are grown in areas with high salt concentrations. If we want to have better visualization and understanding of mangrove ecosystems, mapping the details of mangrove forests is one of the most effective methods (Dhingra and Kumar 2019). In the mangrove ecosystems mapping process, what will be revealed is the detection of changes due to human activities or environmental effects over a long period. Examining the changes in the aerial roots of this ecosystem

Fig. 5 Misclassified pixels of our 10-m map

can indicate the condition of mangrove forests, because these roots will disappear with increasing water levels and sediments (Abburu and Babu Golla 2015). Chips are challenging to collect as training data through field surveys because mangrove forests often grow in swamps and inaccessible areas. New advances in remote-sensing techniques have great potential to overcome the problem of field data acquisition in inaccessible areas of the mangrove ecosystem. In this study, we use mangrove features for efficient mapping using a multi-resolution data set. Images such as Landsat images are more suitable for detecting changes in mangrove canopies. Still, since mangrove forests are usually composed of small fragments, they are not suitable for examining more Landsat data (Shafaey et al. 2019). However, to identify small objects such as single trees and aerial roots, it is helpful to use Sentinel data. This sensor can differentiate between small objects by increasing the number of spectral bands and spatial techniques. Networks with a different level between 20 and 100 ha had the largest number of networks and these networks were scattered throughout the study area. In comparison, networks with a level difference between 0 and 20 ha were mainly seen in the eastern regions. The percentage of networks with surface difference values greater than zero hectares (45%) is similar to areas smaller than zero hectares (51%). Most networks have a distinction between zero and 25 ha, and this difference in the area has made it possible to cover the entire area. The results of extracting mangrove forests in the area from the 10-m and 30-m map showed that mangrove plots with an area of less than 1 ha were not identified in any of the products of the 30-m map, but the same areas were clearly shown in the 10-m map, which shows efficiency. In the 30-m map, salt marshes and narrow rivers were identified as mangrove products. This type of classification is incorrect in 30-m products and provides false information about the extent of mangrove distribution in this area, while there was no such problem in 10-m products. Sentinel-2 has four red-edge strips influenced by the properties and vegetation, looking like water content and leaf chlorophyll, so-called biophysical properties. To find out how sensitive the four red-edge bands of Sentinel-2 are in the extraction of mangrove forests, two scenarios were defined as P1 and P2. With the help of these two scenarios, we determined the classification accuracy.

Table 6 Examine the details of the classification between P1 and P2

Type	F1-score	Producer's accuracy	User's accuracy
P1	0.88	0.91	0.82
P2	0.92	0.89	0.86

In 10-m maps, individual pieces of mangrove are easily monitored. Extraction of the changes in these pieces of mangrove forests can be effective in protecting and helping the growth of this ecosystem. Also, preparing a 10-m map has the advantage that these areas can be covered with the help of strategic protection plans (Kaur et al. 2017). If plants are planted, and these areas are rehabilitated on a 10-m map, the result of protective measures can be observed.

In those studies, the main bands of both Landsat and Sentinel-2 satellites were used to prepare a forest type map. However, the superiority of Sentinel-2 over Landsat was revealed in their research, and the reason for this superiority was the higher spatial resolution of Sentinel-2. And it has more spectral bands compared to the Landsat-8 satellite.

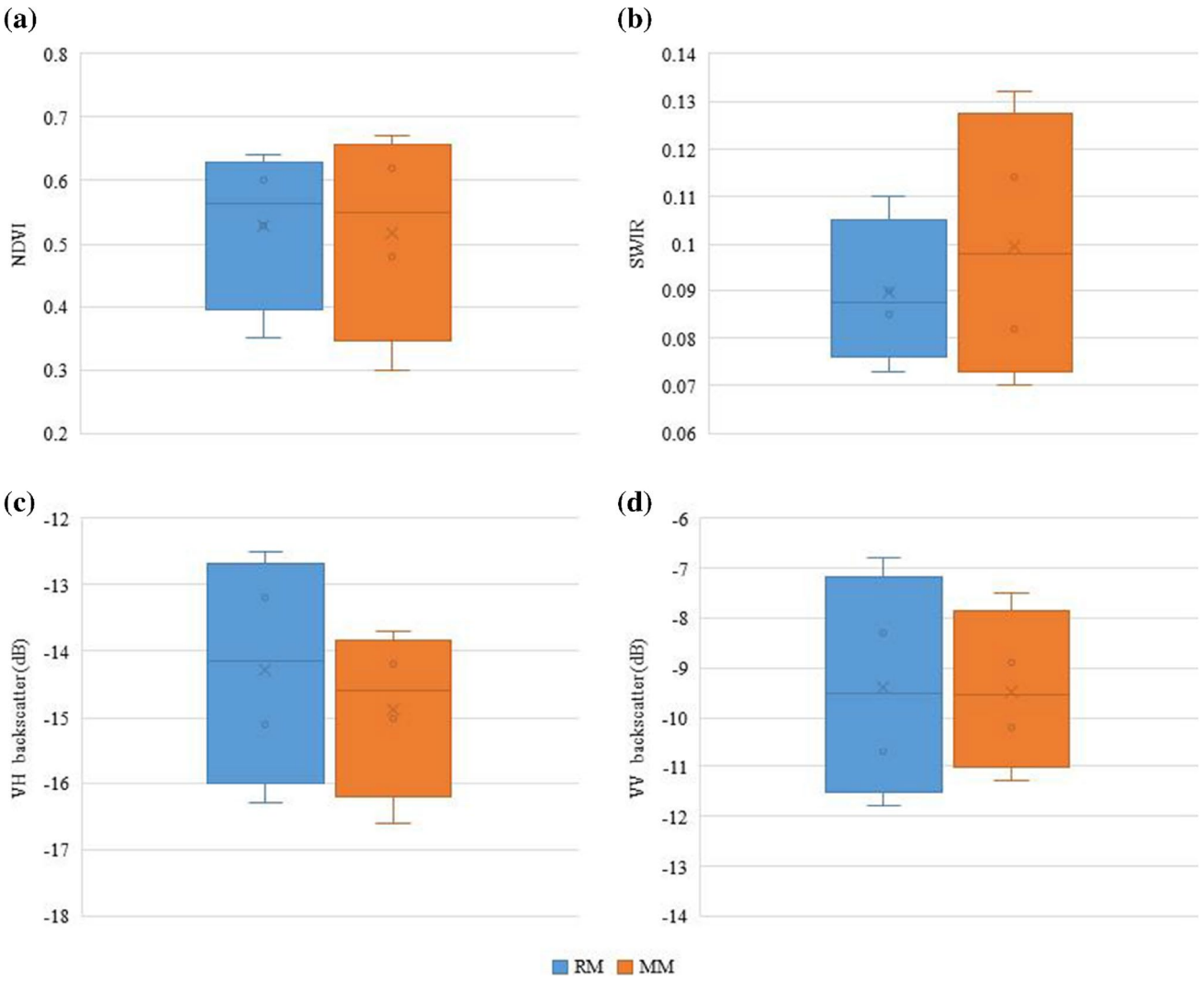

Fig. 6 Boxplots of **a** NDVI, **b** SWIR-1, **c** VH, and **d** VV for mangroves (RM) and misclassified mangroves (MM)

Due to the different spectral characteristics of forest species, it can be expected that by increasing the spectral resolution of satellite images, the possibility of different types of separation will also increase (Belgiu and Drăgu 2016).

Conclusions

In this study, Sentinel-1 and -2 time-series data were used in the GEE platform to detect the progress and regression of mangrove forests in southern Iran. The maps made for spatial monitoring of the study area had a spatial resolution of 10 m. The isolated areas of mangrove forests with an area of less than 1 ha were easily identified with the help of Sentinel time-series images with a spatial resolution of 10 m. It was challenging to study these isolated areas with Landsat images because the spatial resolution of Landsat images is 30 m, it was difficult to monitor these areas with Landsat images, but the use of Sentinel images solved this problem and showed the optimal performance of data from Sentinel images in monitoring changes in isolated mangrove forests in this study. However, the images received from the four red-edge bands of Sentinel-2 had a significant contribution to produce mangrove forests map in south of Iran with a spatial resolution of 10 m. A total of 2400 ha of mangrove forests have been identified in southern Iran. With an area of isolated areas or small patches of less than 1 ha equivalent to 300 ha, mangrove forests in south of Iran account for 12.5% of the total area. Preparing a map of mangrove forests and knowing the area of these forests can be effective in protecting these areas and this research can be used as an effective step for mapping mangrove forests on a global scale based on the processing of Sentinel images on the GEE platform.

Funding This work was supported by Shahid Rajaee Teacher Training University under contract number 19059.

Declarations

Conflict of interest The authors declare that they have competing interests.

References

Abburu S, Babu Golla S (2015) Satellite image classification methods and techniques: a review. Int J Comput Appl. https://doi.org/10.5120/21088-3779

Akhrianti I (2019) Spatial distribution of mangrove in Kelapan Island. Regency, South Bangka

Atwood TB, Connolly RM, Almahasheer H et al (2017) Global patterns in mangrove soil carbon stocks and losses. Nat Clim Chang. https://doi.org/10.1038/nclimate3326

Azmat A, Kazmi JH, Shahzad A, Shaikh S (2020) Mapping change in spatial extent and density of mangrove forests at Karachi Coast using object based image analysis. Int J Econ Environ Geol. https://doi.org/10.46660/ojs.v11i1.423

Badusha AMAA, Mohideen SK (2021) A hybrid ACO based optimized RVM Algorithm for land cover satellite image classification. EAI Endorsed Trans Energy Web. https://doi.org/10.4108/eai.23-12-2020.167789

Belgiu M, Drăgu L (2016) Random forest in remote sensing: a review of applications and future directions. In ISPRSISPRS J Photogramm Remote Sens 114:24–31. https://doi.org/10.1016/j.isprsjprs.2016.01.011

Camisón C, Villar-López A (2014) Organizational innovation as an enabler of technological innovation capabilities and firm performance. J Bus Res. https://doi.org/10.1016/j.jbusres.2012.06.004

Castillo JAA, Apan AA, Maraseni TN, Salmo SG (2017) Estimation and mapping of above-ground biomass of mangrove forests and their replacement land uses in the Philippines using Sentinel imagery. ISPRS J Photogramm Remote Sens. https://doi.org/10.1016/j.isprsjprs.2017.10.016

Chauhan S, Darvishzadeh R, Lu Y et al (2020) Understanding wheat lodging using multi-temporal Sentinel-1 and Sentinel-2 data. Remote Sens Environ. https://doi.org/10.1016/j.rse.2020.111804

De Alban JDT, Jamaludin J, Wong De Wen D et al (2020) Improved estimates of mangrove cover and change reveal catastrophic deforestation in Myanmar. Environ Res Lett. https://doi.org/10.1088/1748-9326/ab666d

Dhingra S, Kumar D (2019) A review of remotely sensed satellite image classification. Int J Electr Comput Eng:1720–1731. https://doi.org/10.11591/ijece.v9i3

Felegari S, Sharifi A, Moravej K et al (2021) Integration of Sentinel 1 and Sentinel 2 satellite images for crop mapping. Appl Sci. https://doi.org/10.3390/app112110104

Friess DA, Rogers K, Lovelock CE et al (2019) The State of the world's mangrove forests: past, present, and future. Annu Rev Environ Resour. https://doi.org/10.1146/annurev-environ-101718-033302

Gao BC (1996) NDWI - a normalized difference water index for remote sensing of vegetation liquid water from space. Remote Sens Environ. https://doi.org/10.1016/S0034-4257(96)00067-3

Ghaderizadeh S, Abbasi-Moghadam D, Sharifi A et al (2021) Hyperspectral image classification using a hybrid 3D-2D convolutional neural networks. IEEE J Sel Top Appl Earth Obs Remote Sens. https://doi.org/10.1109/JSTARS.2021.3099118

Ghasemi S, Javid AH, Farsad F et al (2021) An evaluation of the marine environmental resilience to the north of Qeshm Island. Environ Monit Assess. https://doi.org/10.1007/s10661-021-09627-5

Ghorbanian A, Zaghian S, Asiyabi RM et al (2021) Mangrove ecosystems mapping using Sentinel-1 and Sentinel-2 satellite images and random forest algorithm in google earth engine. Remote Sens. https://doi.org/10.3390/rs13132565

Hill MJ (2013) Vegetation index suites as indicators of vegetation state in grassland and savanna: an analysis with simulated SENTINEL 2 data for a North American transect. Remote Sens Environ. https://doi.org/10.1016/j.rse.2013.06.004

Hu L, Li W, Xu B (2018) Monitoring mangrove forests change in China from 1990 to 2015 using Landsat-derived spectral-temporal variability metrics. Int J Appl Earth Obs Geoinf. https://doi.org/10.1016/j.jag.2018.04.001

Hu P, Sharifi A, Tahir MN et al (2021) Evaluation of vegetation indices and phenological metrics using time-series modis data for monitoring vegetation change in Punjab. Pakistan Water (Switzerland). https://doi.org/10.3390/w13182550

Hurskainen P, Adhikari H, Siljander M et al (2019) Auxiliary datasets improve accuracy of object-based land use/land cover classification in heterogeneous savanna landscapes. Remote Sens Environ. https://doi.org/10.1016/j.rse.2019.111354

Jia M, Wang Z, Wang C, Mao D, Zhang Y (2019) A new vegetation index to detect periodically submerged mangrove forest using single-tide Sentinel-2 imagery. Remote Sens 11(17). https://doi.org/10.3390/rs11172043

Jia SL, Chi Z, Liu GL, et al (2020) Fungi in mangrove ecosystems and their potential applications. Crit. Rev. Biotechnol

Karydas C, Bouarour O, Zdruli P (2020) Mapping spatio-temporal soil erosion patterns in the Candelaro River Basin, Italy, using the G2 model with Sentinel2 imagery. Geosci. https://doi.org/10.3390/geosciences10030089

Kaur A, Sachdeva K, Rani V (2017) A review on satellite image classification. Int J Comput Sci Information Technol 11(1)

Kumar L, Mutanga O (2018) Google Earth Engine applications since inception: usage, trends, and potential. Remote Sens. https://doi.org/10.3390/rs10101509

Li H, Han Y, Chen J (2020) Combination of Google Earth imagery and Sentinel-2 data for mangrove species mapping. J Appl Remote Sens. https://doi.org/10.1117/1.jrs.14.010501

Mazraeh HM, Pazhouhanfar M (2018) Effects of vernacular architecture structure on urban sustainability case study: Qeshm Island. Iran Front Archit Res. https://doi.org/10.1016/j.foar.2017.06.006

Mondal B, Saha AK, Roy A (2021) Spatio-temporal pattern of change in mangrove populations along the coastal West Bengal. Environ Challenges, India. https://doi.org/10.1016/j.envc.2021.100306

Moradi E, Sharifi A (2022) Assessment of forest cover changes using multi-temporal Landsat observation. Environ Dev Sustain. https://doi.org/10.1007/s10668-021-02097-2

Mursyid H, Daulay MH, Pratama AA, Laraswati D, Novita N, Malik A, Maryudi A (2021) Governance issues related to the management and conservation of mangrove ecosystems to support climate change mitigation actions in Indonesia. In Forest Policy Econ 133. https://doi.org/10.1016/j.forpol.2021.102622

Osland MJ, Enwright NM, Day RH, et al (2016) Beyond just sea-level rise: considering macroclimatic drivers within coastal wetland vulnerability assessments to climate change. Glob. Chang. Biol

Robertson AI, Daniel PA, Dixon P (1991) Mangrove forests structure and productivity in the Fly River estuary, Papua New Guinea. Mar Biol. https://doi.org/10.1007/BF01986356

Ronoud G, Fatehi P, Darvishsefat AA et al (2021) Multi-sensor aboveground biomass estimation in the broadleaved Hyrcanian forest of Iran. Can J Remote Sens. https://doi.org/10.1080/07038992.2021.1968811

Sagawa T, Yamashita Y, Okumura T, Yamanokuchi T (2019) Satellite derived bathymetry using machine learning and multi-temporal satellite images. Remote Sens. https://doi.org/10.3390/rs11101155

Sekulić A, Kilibarda M, Heuvelink GBM et al (2020) Random forest spatial interpolation. Remote Sens. https://doi.org/10.3390/rs12101687

Shafaey MA, Salem MAM, Ebied HM, Al-Berry MN, Tolba MF (2019) Deep Learning for Satellite Image Classification. Adv Intell Sys Comput 845:383–391. https://doi.org/10.1007/978-3-319-99010-1_35

Sidik F, Supriyanto B, Krisnawati H, Muttaqin MZ (2018) Mangrove conservation for climate change mitigation in Indonesia. In Wiley interdisciplinary reviews: Clim Chang 9(5). https://doi.org/10.1002/wcc.529

Tan FL, Ye GF, Cui LJ et al (2010) Site type classification of mongrove in Quanzhou estuary wetlands. Wetl Sci 8:366–370

Tariq A, Shu H, Siddiqui S et al (2022) Spatio-temporal analysis of forest fire events in the Margalla Hills, Islamabad, Pakistan using socio-economic and environmental variable data with machine learning methods. J For Res. https://doi.org/10.1007/s11676-021-01354-4

Thiagarajan K, Anandan MM, Stateczny A et al (2021) Satellite image classification using a hierarchical ensemble learning and correlation coefficient-based gravitational search algorithm. Remote Sens. https://doi.org/10.3390/rs13214351

Toosi NB, Soffianian AR, Fakheran S, Waser LT (2022) Mapping disturbance in mangrove ecosystems: incorporating landscape metrics and PCA-based spatial analysis. Ecol Indic. https://doi.org/10.1016/j.ecolind.2022.108718

Tucker CJ (1979) Red and photographic infrared linear combinations for monitoring vegetation. Remote Sens Environ. https://doi.org/10.1016/0034-4257(79)90013-0

Twilley RR, Rovai AS, Riul P (2018) Coastal morphology explains global blue carbon distributions. Front Ecol Environ. https://doi.org/10.1002/fee.1937

Vaiphasa C, Ongsomwang S, Vaiphasa T, Skidmore AK (2005) Tropical mangrove species discrimination using hyperspectral data: a laboratory study. Estuar Coast Shelf Sci. https://doi.org/10.1016/j.ecss.2005.06.014

Van der Stocken T, Carroll D, Menemenlis D et al (2019) Global-scale dispersal and connectivity in mangroves. Proc Natl Acad Sci USA. https://doi.org/10.1073/pnas.1812470116

Wachid MN, Hapsara RP, Cahyo RD, Wahyu GN, Syarif AM, Umarhadi DA, Fitriani AN, Ramadhanningrum DP, Widyatmanti W (2017) Mangrove canopy density analysis using Sentinel-2A imagery satellite data. IOP conference series: Earth Environ Sci 70(1). https://doi.org/10.1088/1755-1315/70/1/012020

Wessel M, Brandmeier M, Tiede D (2018) Evaluation of different machine learning algorithms for scalable classification of tree types and tree species based on Sentinel-2 data. Remote Sens. https://doi.org/10.3390/rs10091419

Xu H (2006) Modification of normalised difference water index (NDWI) to enhance open water features in remotely sensed imagery. Int J Remote Sens. https://doi.org/10.1080/01431160600589179

Zhang W, Brandt M, Wang Q et al (2019) From woody cover to woody canopies: how Sentinel-1 and Sentinel-2 data advance the mapping of woody plants in savannas. Remote Sens Environ. https://doi.org/10.1016/j.rse.2019.111465